J. Phys.: Condens. Matter **21** (2009) 385501 (4pp) doi:10.1088/0953-8984/21/38/385501

Crystal lattice and band structure of the intermediate high-pressure phase of PbSe

S V Streltsov[1], A Yu Manakov[2], A P Vokhmyanin[1], S V Ovsyannikov[1] and V V Shchennikov[1]

[1] Institute of Metal Physics, 18 S. Kovalevskaya Street, 620041 Ekaterinburg GSP-170, Russia
[2] A V Nikolaev Institute of Inorganic Chemistry, Novosibirsk 630090, Russia

E-mail: streltsov.s@gmail.com

Received 22 May 2009, in final form 6 July 2009
Published 24 August 2009
Online at stacks.iop.org/JPhysCM/21/385501

Abstract

In the present paper the results of fitting synchrotron diffraction data are obtained for the intermediate high-pressure phase (9.5 GPa) of the lead selenide based compound $Pb_{1-x}Sn_xSe$ ($x = 0.125$)—an optoelectronic as well as a thermoelectric material—for two types of lattice symmetries *Pnma* (space group #62) and *Cmcm* (space group #63). Both lattice parameters and positions of atoms for the above mentioned structures have been used in calculations of the electron structure of high-pressure phases. The main difference between the electronic properties for *Cmcm* and *Pnma* structures established in electronic structure calculations is that in the first one the PbSe compound was found to be a metal, while in the second a small semiconductor gap ($E_G = 0.12$ eV) was obtained. Moreover, the forces in the *Cmcm* structure are an order of magnitude larger than those calculated for the *Pnma* lattice. In the optimized, *Pnma* structure within a generalized gradient approximation (GGA), the band gap increases up to $E_G = 0.27$ eV. The result coincides with the data on thermoelectric power and electrical resistance data pointing to a semiconductor gap of ∼0.2 eV at ∼9.5 GPa. Thus, the *Pnma* type of lattice seems to be a preferable version for the intermediate phase compared with the *Cmcm* one.

(Some figures in this article are in colour only in the electronic version)

1. Introduction

At ambient conditions the narrow gap infrared laser as well as the thermoelectric semiconductor PbSe crystallizes in the sixfold-coordinated NaCl-type structure (B1, space group $Fm\bar{3}m$) [1]. Early high-pressure investigations by x-ray diffraction and electrical transport methods have shown that lead chalcogenides PbX (X—Te, Se, S) undergo a set of similar structural phase transitions [2–14]. At pressures of 13–25 GPa, all lead chalcogenides PbX adopt the eightfold-coordinated CsCl-type structure (B2, $Pm\bar{3}m$), where they are reported to be metallic and superconducting [2, 3, 5, 15, 16]. At intermediate pressures of 2.5–6 GPa, the PbX transform to orthorhombic phases. Three different structure types, namely, GeS (B16, *Pnma*), FeB (B27, *Pnma*) and CrB/TlI (B33, *Cmcm*), have been proposed for these intermediate phases [4–11, 13, 14, 17]. A detailed transition pathway from the B1 to the B2 structure via intermediate orthorhombic phases has been considered in [18–20]. Only recently has the structure of the above mentioned intermediate phases been certainly established for PbTe compounds to be the *Pnma* type [13, 21]. The crystal structure of the intermediate high-pressure phase of PbSe, in spite of recent synchrotron investigations [14, 22], still remains unclear. Interest in the high-pressure phases of lead chalcogenides is now enhanced due to proposed excellent thermoelectric properties of those found for PbTe (as well as for high-pressure phases of other chalcogenides, e.g. HgTe [23, 24], Bi_2Te_3 [25]) both in experiments [26] and in theoretical calculations [27].

In the present paper a synchrotron study of the intermediate phase of PbSe has been performed at a pressure of ∼9.5 GPa, and the electronic band structure has been calculated based on the structural parameters for detailing the type of the high-pressure intermediate phase. This allowed us to find that *Pnma* symmetry is more suitable for the description of a given phase and provides a reliable crystal structure for it. Improved thermoelectric properties are expected for the high-

Table 1. Crystal structure of PbSe obtained at $P \approx 9.5$ GPa using x-ray high-pressure synchrotron data (see the text), and the parameters obtained for the *Pnma* lattice after optimization within the generalized gradient approximation (GGA).

Space group	*Cmcm*	*Pnma*	*Pnma* (optimized)
Lattice parameters	$a = 4.06$	$a = 11.187(6)$	$a = 11.1876$
Parameters (Å)	$b = 10.85$	$b = 4.174(8)$	$b = 4.1748$
	$c = 4.16$	$c = 4.059(8)$	$c = 4.0598$
Positions of atoms	Pb(0, 0.07, 1/4)	Pb(0.1334, 1/4, 0.0158)	Pb(0.1176, 1/4, 0.0009)
	Se(0, 0.30, 1/4)	Se(0.1201, 3/4, 0.5047)	Se(0.13533, 3/4, 0.50026)

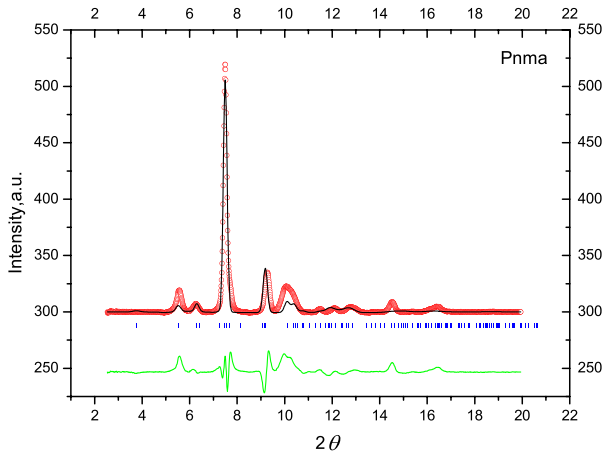

Figure 1. Diffraction pattern for $Pb_{0.875}Sn_{0.125}Se$ crystal at 9.5 GPa with fittings to the *Pnma* lattice.

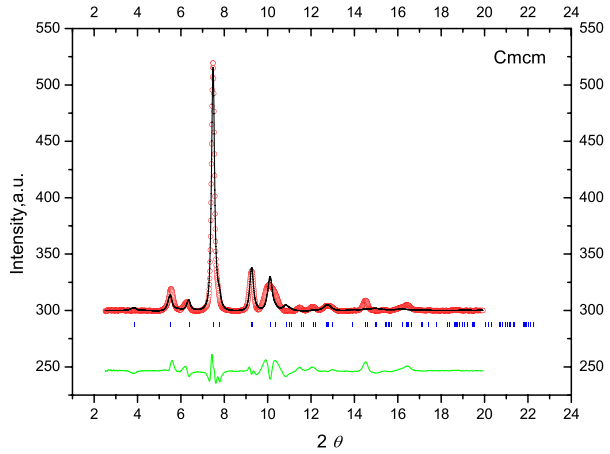

Figure 2. Diffraction pattern for $Pb_{0.875}Sn_{0.125}Se$ crystal at 9.5 GPa with fittings to the *Cmcm* lattice.

pressure intermediate phase of PbSe, analogously to the one obtained for the PbTe high-pressure phase [26].

2. Experiment and calculation details

The measurements have been carried out at room temperature in a window diamond anvil cell (DAC) on a station of the fourth channel of the VEPP-3 accelerator (at the Siberian Synchrotron and Terahertz Radiation Center, Budker Institute of Nuclear Physics SB, RAS) in 0.3675 Å monochromatic synchrotron radiation. An MAR-3450 image plate detector was used to detect the diffracted radiation. A sample was placed in a hole of ∼0.2 mm diameter in a stainless-steel compressible gasket. The pressure in a methanol–ethanol (4:1) transmitting medium was determined by the equation of state of Ag [28, 29] and also from the shift of the ruby luminescence line. The diffraction data were analyzed by means of the FULLPROF program for the profile analysis (the Rietveld method). For an improvement in image detail at the diffraction pattern, moderate laser heating of the sample under pressure has been performed before measurements.

The band structure calculations were carried out in pseudopotential code PW-SCF [30], with the use of ultrasoft pseudopotentials with the Perdew–Burke–Ernzerhof (PBE) version of the exchange potential [31]. The plane-wave and kinetic energy cut-offs were chosen to be 40 Ryd and 180 Ryd, respectively. A mesh of 144 k-points in the Brillouin-zone was used for the calculation. Then crystal structure optimization was performed, while the forces were more than 2 mRyd au^{-1}.

The experimental crystal structure parameters used for the calculation have been obtained from fitting the experimental diffraction patterns using the FULLPROF program for various types of lattices (see table 1).

In order to check the accuracy of the computational scheme we tested it on the $P = 0$ GPa NaCl structure of PbSe [32]. Experimentally the band gap in PbSe at these conditions is 0.27 eV [33], while in the calculation we obtained 0.39 eV. It means that one may estimate the accuracy of the method ∼0.12 eV.

3. X-ray diffraction (XRD) results

The XRD experiments were performed on three samples of $Pb_{0.875}Sn_{0.125}Se$. The NaCl lattice was found to persist to at least 7.28 GPa; at 2.21, 2.37, 6.01 and 7.28 GPa its lattice parameter a was equal respectively to: 6.0337, 6.0007, 5.926 and 5.897 Å. The Rietveld refinement of the XRD patterns at $P \approx 9.5$ GPa is assigned to the intermediate phase. It turns out that approximately similar results of fittings have been obtained for two various types of lattice of the intermediate phase (figures 1 and 2). Thus, for the intermediate phase of $Pb_{0.875}Sn_{0.125}Se$ at ∼9.5 GPa we established the TlI (*Cmcm* space group) and GeS structural types (*Pnma* space group) [22]. Lattice parameters and atom positions for both symmetries are presented in table 1.

The lattice parameters used in calculations for both structures are rather similar: $a_{Cmcm} \approx c_{Cmcm} \approx b_{Pnma} \approx c_{Pnma} \approx$ and $b_{Cmcm} \approx a_{Pnma}$ [14].

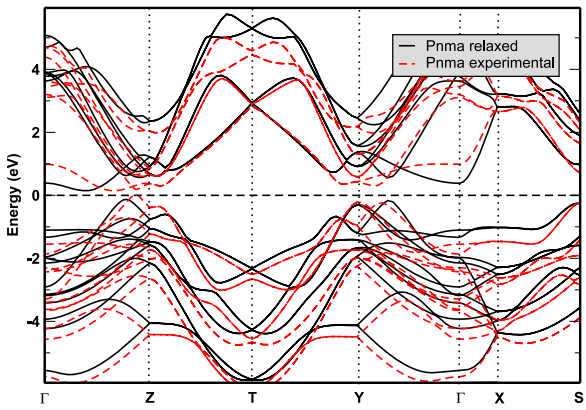

Figure 3. Band structures obtained in GGA calculations for experimental (black, solid) and relaxed crystal structures (red, dashed) of PbSe within *Pnma* symmetry. The Fermi energy is at zero energy.

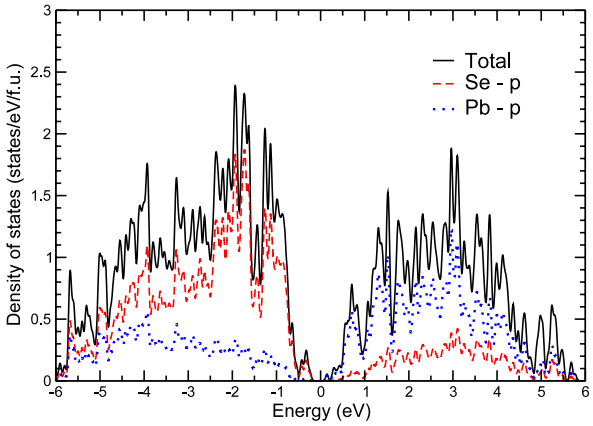

Figure 4. Total and partial density of states (DOS), obtained in the GGA calculation after relaxation of the experimental structure corresponding to *Pnma* symmetry. The Fermi energy is at zero energy.

4. Results of band structure calculations

The positions of the atoms, obtained by different fittings and summarized in table 1, were used as input parameters in our calculations for PbSe. The influence of the substitution of a small minority of Pb by Sn atoms in the cation sub-lattice were taken into account by the real lattice parameters of the binary compound.

The main difference between the electronic properties for *Cmcm* and *Pnma* structures established in our electron structure calculations is that in the first one PbSe was found to be a metal, while in the second a small semiconductor gap ($E_G = 0.12$ eV) was obtained. The total force in the *Cmcm* solution equals 0.274 Ryd au^{-1}, while it is only 0.038 Ryd au^{-1} for the *Pnma* structure. Thus, one can see that the crystal structure obtained in the refinement procedure within the *Cmcm* symmetry does not correspond to an equilibrium crystal structure. The forces acting on Pb and Se atoms are equally large in the *Cmcm* structure: $F_{Pb} = 0.159$ Ryd au^{-1}, $F_{Se} = 0.112$ Ryd au^{-1}.

The band structure obtained for the *Pnma* structure is presented in figure 3. One may notice that the band gap is indirect, but it is only ∼0.04 eV smaller than the direct one. An analysis of partial contributions to the density of states (DOS) presented in figure 4 shows that the top of the valence band is mostly defined by Se p states, while the bottom of the conduction band by Pb p states.

It is interesting that the band structure for the *Pnma* structure in the vicinity of the Fermi level is strongly modified after optimization of the structure. For the optimization we assumed that the lattice constants and the whole symmetry was safety defined in x-ray experiments. Thus only the positions of atoms were allowed to be varied in the optimization process, which was carried out in the framework of the Broyden–Fletcher–Goldfarb–Shanno algorithm [34]. The resulting crystal structure parameters are presented in table 1, while the comparison between band structures obtained for the experimental and optimized crystal structures can be found in figure 3 (DOS for the optimized crystal structures is presented in figure 4).

In the *Pnma* optimized structure the bonding–antibonding Pb–Se splitting increases significantly. This results in a larger band gap, $E_G = 0.27$ eV, which becomes clearly indirect, because in the optimized *Pnma* structure Pb p bands are lifted up in the high symmetry Z and Y k-points compared with those obtained for the experimental *Pnma* lattice. This agrees with the experimental estimation of the band gap, as will be discussed further.

For completeness we carried out the optimization of the *Cmcm* structure with experimental lattice parameters as well, but found that its total energy is 9.7 mRyd/f.u. higher than the *Pnma* one. This again indicates that at a pressure of ∼9.5 GPa, the *Pnma* structure seems more favorable than the *Cmcm* one. However, this result is still obtained using experimental lattice parameters, which first of all cannot be eigen (i.e. does not correspond to the lowest total energy) for the density function calculations, and secondly may suffer from uncertainty in fitting x-ray diffraction patterns under pressure.

In order to get a more general result we performed the calculation, where both lattice parameters and atomic coordinates were allowed to be relaxed, but the system was squeezed by an external pressure of ≈9.5 GPa. This, fully independent from experimental data, numerical simulation shows that at pressures of ∼9.5 GPa the *Pnma* structure still has a lower total energy (on 2.3 mRyd/f.u.) than the *Cmcm* one and hence should be realized in the real experiment. The volume of the unit cell in the *Cmcm* structure turns out to be 1.2% smaller than in the *Pnma* one.

5. Discussion

The synchrotron diffraction data obtained in the present work, as well as those published in [14, 22], do not allow an unambiguous choice of the type of lattice for the intermediate phase of the PbSe compound. Thus, both *Pnma* and *Cmcm* ones give almost an equivalent fitting of the experimental data (figures 1 and 2). An attempt has been performed to detail the type of lattice using the Raman scattering technique [35, 36], as selection rules for it depend strongly on the symmetry of

crystal [37]. But in the experiments only a few Raman peaks have been observed, much less than in both lattices proposed for the intermediate phase [35, 36]. Electronic structure calculations performed in the present work give an additional opportunity to make a choice. They show that the *Cmcm* crystal structure is far from the equilibrium one, and also provide the band gap value for the *Pnma* crystal structure close to the experimental value. Indeed, the data on the thermoelectric power and resistivity both suggest the intermediate phase of the PbSe compound to be a narrow gap semiconductor with a semiconductor gap $E_G \sim 0.4$ eV at ~5 GPa [12, 14, 16, 17]. Under pressure the gap narrows and at $P = 9.5$ GPa the estimated value is $E_G \sim 0.2$ eV [14]. The transition to a metal state occurs only at the next high-pressure CsCl-phase [5, 16].

It is interesting to compare the electron structure of the intermediate high-pressure orthorhombic phases of PbSe and PbTe [27]. In both cases there are indirect semiconductor gaps E_G which are only lower than the direct ones by a small amount. However, in the case of PbTe the orthorhombic phase has a narrow semiconductor gap $E_G = 0.17$ eV (at ~6.5 GPa) [14, 27] providing excellent thermoelectric properties [26, 27]. The anisotropy of the electronic structure is responsible the high thermoelectric parameters found in experiment [26] and confirmed by theoretical calculations [27]. For the PbSe compound the thermoelectric parameters of orthorhombic high-pressure phase at room temperature are found to be low because of a relatively high electrical resistivity [16, 17, 26]. For PbTe the increase of temperature tends to enlarge the thermoelectric figure of merit Z in the orthorhombic phase, so a high-pressure phase of PbSe compounds may still be considered as a prospective thermoelectric material thanks to the low value of semiconductor gap of indirect type, as in the case of PbTe [38]. The intermediate high-pressure phases of both PbTe and PbSe, which are found to be narrow gap semiconductors, may also be proposed as potential infrared laser materials like the initial NaCl-phases of these compounds.

Acknowledgments

The authors are grateful to A Efremov, who performed preliminary calculations within the linear muffin-tin orbital calculations. The work was supported by the Dynasty Foundation and International Center for Fundamental Physics in Moscow, by the Russian Ministry of Science and Education via program 02.740.11.0217 and together with the Civil Research and Development Foundation through grant Y4-P-05-15, by the Russian Foundation for Basic Research through RFFI-07-02-00041, and RFFI-07-08-00338. Additionally the support of the Ural division of the Russian Academy of Science is acknowledged.

References

[1] Ravich Y I, Efimova B A and Smirnov I A 1970 *Semiconducting Lead Chalcogenides* (New York: Plenum)
[2] Samara G A and Drickamer H G 1962 *J. Chem. Phys.* **37** 1159
[3] Semerchan A A, Kuzin N N, Drozdova L N and Vereshchagin L F 1963 *Dokl. Akad. Nauk SSSR* **152** 107
[4] Wakabayashi J, Kobayashi H, Nagasaki H and Minomura S 1968 *J. Phys. Soc. Japan* **25** 227
[5] Brandt N B, Gitsu D V, Popovich N S, Sidorov V I and Chudinov S M 1975 *JETP Lett.* **22** 104
[6] Volkov B A, Kucherenko I V, Moiseenko V N and Shotov A P 1978 *JETP Lett.* **27** 371
[7] Chattopadhyay T, Von Schnering H G, Grosshans W A and Halzapfel W B 1986 *Physica* B + C **139/140** 356
[8] Ves S, Pusep Y A, Syassen K and Cardona M 1989 *Solid State Commun.* **70** 257
[9] Maclean J *et al* 1995 *Nucl. Instrum. Methods Phys. Res.* B **97** 354
[10] Ahuja R 2003 *Phys. Status Solidi* b **235** 341
[11] Knorr K, Ehm L, Hytha M, Winkler B and Depmeier W 2003 *Eur. Phys. J.* B **31** 297
[12] Ovsyannikov S V, Shchennikov V V, Ponosov Y S, Gudina S V, Guk V G, Skipetrov E P and Mogilenskikh V E 2004 *J. Phys. D: Appl. Phys.* **37** 1151
[13] Rousse G, Klotz S, Saitta A M, Rodriguez-Carvajal J, McMahon M I, Couzinet B and Mezouar M 2005 *Phys. Rev.* B **71** 224116
[14] Ovsyannikov S V, Shchennikov V V, Manakov A Y, Likhacheva A Y, Ponosov Y S, Mogilenskikh V E, Vokhmyanin A P, Ancharov A I and Skipetrov E P 2009 *Phys. Status Solidi* b **246** 615
[15] Timofeev Y A, Vinogradov B V and Yakovlev E N 1981 *Sov. Phys.—Solid State* **23** 1474
[16] Ovsyannikov S V, Shchennikov V V, Popova S V and Derevskov A Yu 2003 *Phys. Status Solidi* b **235** 521
[17] Shchennikov V V, Ovsyannikov S V and Derevskov A Yu 2002 *Phys. Solid State* **44** 1845
[18] Toledano P, Knorr K, Ehm L and Depmeier W 2003 *Phys. Rev.* B **67** 144106
[19] Stokes H T, Hatch D M, Dong J J and Lewis J P 2005 *Phys. Rev.* B **69** 174111
[20] Zahn D and Leoni S 2004 *Phys. Rev. Lett.* **92** 250201
[21] Shchennikov V V, Ovsyannikov S V, Manakov A Yu, Likhacheva A Yu, Ancharov A I, Berger I F and Sheromov M A 2006 *JETP Lett.* **83** 228
[22] Ovsyannikov S V, Shchennikov V V, Manakov A Y, Likhacheva A Y, Berger I F, Ancharov A I and Sheromov M A 2007 *Phys. Status Solidi* b **244** 279
[23] Chen X, Wang Y, Cui T, Ma Y, Zou G and Iitaka T 2008 *J. Chem. Phys.* **128** 194713
[24] Shchennikov V V, Gavaleshko N P and Frasunyak F M 1995 *Fiz. Tverd. Tela* **37** 3532
[25] Ovsyannikov S V, Shchennikov V V, Vorontsov G V, Manakov A Y, Likhacheva A Y and Kulbachinskii V A 2008 *J. Appl. Phys.* **104** 053713
[26] Ovsyannikov S V and Shchennikov V V 2007 *Appl. Phys. Lett.* **90** 122103
[27] Wang Y, Chen X, Cui T, Niu Y, Wang Y, Wang M, Ma Y and Zou G 2007 *Phys. Rev.* B **76** 155127
[28] Goryainov S V and Belitsky I A 1995 *Phys. Chem. Minerl.* **22** 443
[29] Ancharov A I, Manakov A Y and Mezentsev N A *et al* 2001 *Nucl. Instrum. Methods Phys. Res.* A **470** 80
[30] Baroni S *et al PWSCF (Plane-Wave Self-consistent Field) Codes* http://www.pwscf.org
[31] Perdew J P, Burke K and Ernzerhof M 1996 *Phys. Rev. Lett.* **77** 3865
[32] Earley J W 1950 *Am. Minerl.* **35** 337
[33] Ravich Yu I, Efimova B A and Smirnov I A 1968 *Methods of Semiconductor Investigations in Application to Lead Chalcogenides PbTe, PbSe, PbS* (Moscow: Nauka) p 384
[34] Fletcher R 1987 *Practical Methods of Optimization* (Chichester: Wiley)
[35] Ponosov Y S, Ovsyannikov S V, Shchennikov V V and Mogilenskikh V E 2007 *J. Phys. Soc. Japan* **76** (suppl. A) 15
[36] Ponosov Yu S, Ovsyannikov S V, Streltsov S V, Shchennikov V V and Syassen K 2009 *High Pressure Res.* **29** 224
[37] Yu P and Cardona M 2002 *Fundamentals of Semiconductors* (New York: Springer)
[38] Shchennikov V V and Ovsyannikov S V 2003 *Solid State Commun.* **126** 373